Research Square

Preprints are preliminary reports that have not undergone peer review.
They should not be considered conclusive, used to inform clinical practice,
or referenced by the media as validated information.

Comparative tentacle transcriptomics reveals candidate chemosensory receptors in the gray field slug Deroceras reticulatum

Seung-Joon Ahn
Mississippi State University
Hyo Sang Jang
Oregon State University
Rory Mc Donnell
Oregon State University
Man-Yeon Choi
man-yeon.choi@usda.gov

USDA-ARS

Research Article

Keywords: Transcriptome, Chemosensory Receptor, GPCR, Tentacles, Gray garden slug, Deroceras reticulatum

Posted Date: November 13th, 2026

DOI: https://doi.org/10.21203/rs.3.rs-11600392/v1

License: This work is licensed under a Creative Commons Attribution 4.0 International License.
Read Full License

Additional Declarations:
No competing interests reported.

Tables 1 and 2 are available in the Supplementary Files section.

Comparative tentacle transcriptomics reveals candidate chemosensory receptors in the gray field slug *Deroceras reticulatum*

Seung-Joon Ahn[1], Hyo Sang Jang[2], Rory Mc Donnell[3], Man-Yeon Choi[4,*]

1 Department of Biochemistry, Nutrition, and Health Promotion, Mississippi State University, Starkville, MS 39762, USA

2 Department of Horticulture, Oregon State University, Corvallis, OR 97331, USA

3 Department of Crop and Soil Science, Oregon State University, Corvallis, OR 97331, USA

4 USDA-ARS, Horticultural Crops Disease and Pest Management Research Unit, Corvallis, OR 97331, USA

* Corresponding author: Man-Yeon Choi (man-yeon.choi@usda.gov)

Short title: Chemosensory Receptors in the Slug Tentacles

Keywords: Transcriptome, Chemosensory Receptor, GPCR, Tentacles, Gray garden slug, *Deroceras reticulatum*

Abstract: Chemosensation is essential for foraging, predator avoidance, and reproductive behavior in terrestrial gastropods. The gray field slug (*Deroceras reticulatum*) is a globally important agricultural pest, yet the peripheral molecular mechanisms driving its chemosensory behavior remain poorly understood. Here, we generated and analyzed *de novo* transcriptomes of the upper posterior tentacles (PT) and lower anterior tentacles (AT), using non-sensory mantle tissue (MT) as a comparative baseline. Illumina sequencing and *de novo* assembly yielded 142,526 transcripts, of which 28,310 were functionally annotated. Tissue distribution and differential expression analyses revealed marked molecular specialization between the two tentacle pairs. PT-enriched transcripts were associated with aerial olfaction and photoreception, including neural signaling components, retinal-associated genes, and G protein-coupled receptors (GPCRs), whereas AT-enriched transcripts were associated with contact chemoreception and substrate-associated sensing, with enrichment of structural remodeling components, acetylcholine receptors, and metabolic enzymes. Targeted gene-family mining showed that GPCRs dominated the annotated chemosensory repertoire. A multistep bioinformatic filtering pipeline identified 67 PT-enriched and 38 AT-enriched candidate chemosensory GPCRs, including numerous uncharacterized or orphan receptors. Non-GPCR candidate families included ionotropic glutamate receptors, degenerin/amiloride-sensitive sodium channels, lipocalins, and Niemann-Pick type C2 proteins. qRT-PCR analysis of 17 high-priority candidate GPCRs largely supported the RNA-Seq expression patterns. Together, these tissue-specific profiles provide a molecular resource for understanding slug chemosensory biology and for prioritizing candidate targets for future behavior-based or molecular pest-management strategies.

BACKGROUND

Terrestrial snails and slugs possess two distinct pairs of cephalic tentacles that serve important sensory functions (Chase, 1986). The posterior tentacles (also known as the ocular tentacles) are elongated and dorsally positioned, which likely enhance their ability to detect airborne odorants, and each bears a light-sensitive structure at its apex. In contrast, the anterior tentacles (also known as the peduncular tentacles) are shorter, located near the mouthparts, and thought to be specialized for detecting substrate- and food-associated chemical cues during locomotion (Brenzinger et al., 2021). These tentacles constitute the principal chemosensory organs in gastropods and play essential roles in feeding, orientation, and reproductive behaviors (Chase and Croll, 1981; Ito et al., 2000). Odor molecules are detected by the olfactory epithelium covering the tentacle surface, and sensory information is subsequently transmitted to the tentacular ganglion located beneath the tentacle tip and then relayed to the procerebrum, the secondary olfactory center in the molluscan brain (Chase and Tolloczko, 1993; Ucciferri and Wyeth, 2023).

Chemosensory perception in vertebrates and invertebrates is primarily mediated by large multigene receptor families, many of which encode proteins with a characteristic seven-transmembrane (7-TM) structure (Mombaerts, 1999). Among them, G protein-coupled receptors (GPCRs) represent one of the most ancient and expansive receptor superfamilies in animals (Krishnan and Schiöth, 2015). GPCRs transduce extracellular signals across the plasma membrane through heterotrimeric G-protein complexes and regulate a broad range of physiological and behavioral processes (Weis and Kobilka, 2018). Although vertebrate and arthropod chemoreceptors both possess a 7-TM structure, they are evolutionarily unrelated, exhibiting opposite membrane topologies and distinct signal transduction mechanisms (Hanlon and Andrew, 2015). The independent evolutionary origins of chemosensory receptor systems underscore the importance of investigating these gene families across diverse invertebrate lineages, including Mollusca, the second-largest animal phylum (Xu et al., 2025). In particular, gastropod mollusks provide an important comparative framework for understanding the evolution and diversification of chemosensory GPCRs (Rondón et al., 2024).

GPCR repertoires vary substantially among animal taxa. Approximately 800 GPCR genes have been identified in the human genome (Fredriksson et al., 2003), whereas more than 700 have been reported in the zebrafish, *Danio rerio* (Harty et al., 2015). In invertebrates, the fruit fly *Drosophila melanogaster* possesses more than 200 GPCR genes (Brody and Cravchik, 2000), whereas the nematode *Caenorhabditis elegans* contains approximately 1,300 putative chemosensory GPCRs, representing over 5% of its genome (Vidal et al., 2018). In mollusks, however, GPCR-related studies remain relatively limited. Previous investigations have characterized GPCR families in several molluscan species (Morishita, 2017). For example, in the sea slug, *Aplysia californica*, numerous GPCRs have been identified from the rhinophore, a specialized chemosensory organ (Cummins et al., 2009b). In the aquatic snail, *Biomphalaria glabrata*, several ionotropic glutamate receptors (iGluRs) have been implicated in odor detection (Liang et al., 2016). More recently, comparative genomic analyses revealed substantial expansion of chemosensory GPCR families in terrestrial gastropods. More than 600 Class-A GPCRs were identified in *Arion vulgaris*, a terrestrial slug species inhabiting moist environments, whereas reduced chemosensory repertoires were observed in species adapted to drier habitats (Nath et al., 2025). These findings suggest that habitat diversification may have strongly influenced the evolution of chemosensory receptor systems in terrestrial mollusks. Nevertheless, the molecular basis of chemosensation in many terrestrial slug species, including *Deroceras reticulatum*, remains poorly understood.

The gray field slug, *Deroceras reticulatum* (Müller) (Gastropoda: Pulmonata), is a globally distributed terrestrial pest species native to Europe and now widespread throughout North America and other temperate regions (CABI, 2022; Godan, 1983; Howlett, 2012; Tulli et al., 2009). This species causes significant damage to a wide range of agricultural and horticultural crops (Howlett, 2012; Port and Port, 1989). Adult slugs can reach a length of 3.5–5 cm when crawling and are usually gray or cream in color with characteristic reticulated dark markings. When disturbed, they secrete a milky-white mucus (Mc Donnell et al., 2024). Eggs are generally deposited beneath stones, leaf litter, or within soil crevices, and hatch within several weeks depending on environmental conditions such as temperature and humidity

(South, 1992). *D. reticulatum* is hermaphroditic, with individuals possessing both male and female reproductive organs, although cross-fertilization is common (Runham, 1978).

Current management strategies rely primarily on chemical molluscicide baits, supplemented by cultural practices such as tillage while biological control agents such as parasitic nematodes in the genus *Pellioditis* are used in some parts of the world (Barker, 2002, 2004; Dively and Patton, 2022; Glen and Symondson, 2003; Tan and Grewal, 2001). Consequently, previous studies on *D. reticulatum* have focused mainly on its ecology, pest status, and control measures (Arias, 1960; Howlett, 2005; Iglesias et al., 2002; Lovett and Black, 1920). Early studies examined chemoreception and feeding behaviors of *D. reticulatum* (Frain, 1980; Stephenson, 1979), but the molecular mechanisms remain poorly characterized, mainly due to limited molecular resources for this species. Recent studies have advanced our understanding of slug biology through whole-body transcriptome sequencing with complex neuropeptide repertoires (Ahn et al., 2017) and functional characterization of the first molluscan ortholog of the vertebrate neuromedin U receptor in *D. reticulatum* (Ahn et al., 2020). For potential applications in slug managements, GPCR-targeted bioactive peptides have been identified and shown to exert deterrent effects in this species (Choi et al., 2024). In addition, immune-related gene expression profiles in *D. reticulatum* responding to parasitic nematode infection have also been investigated (Hafeez et al., 2024). Despite these advancements, molecular investigations into the specific physiological roles and sensory modalities of the slug tentacles remain largely unexplored in *D. reticulatum*.

In this study, we analyzed the tentacle transcriptomes of *D. reticulatum*, generated using the Illumina HiSeq 2500 platform. Posterior and anterior tentacles were excised separately, and their transcriptomic profiles were compared with those of the mantle tissue through differential gene expression analysis. Particular emphasis was placed on identifying GPCRs and other chemosensory-related genes enriched in tentacular tissues. The expression patterns of selected candidate genes were further validated by qRT-PCR. Ultimately, these tissue-specific molecular blueprints not only deepen our understanding of gastropod neurobiology and sensory physiology, particularly chemoreception, but also provide a valuable

genetic foundation for identifying relevant chemoreceptor targets and developing next-generation behavioral disruptors for sustainable pest management.

MATERIALS AND METHODS

Slug tentacle and mantle tissue samples, and RNA isolation

Deroceras reticulatum were collected in Corvallis, Oregon, USA (44.567862 N, -123.288672 E). Prior to tissue harvesting, individuals were maintained alive in plastic containers with lettuce and carrot, and damp paper towel at 14 °C. A pair of posterior tentacles (PT) and a pair of anterior tentacles (AT) (Fig. 1A) were precisely excised from each slug using sterilized micro-dissection scissors (Fine Science Tools Inc., Foster City, CA). As a comparative control, a piece of mantle tissue (MT)—devoid of tentacles and internal visceral organs—was separately collected. The mantle is a saddle-shaped piece of tissue located behind the slug head (Mc Donnell et al., 2024). To ensure sufficient biomaterial for downstream application, the tentacle tissue samples were pooled from five individual slugs.

Total RNA was isolated from the three tissue samples, PT, AT, and MT, using PureLink Total RNA Mini Kit (Thermo Fisher Scientific, Waltham, MA) following the manufacturer's protocol. To eliminate potential genomic DNA contamination, the isolated RNA samples were treated with TURBO DNase (Thermo Fisher Scientific) for 30 min at 37 °C. The treated RNA was subsequently purified by using the RNeasy MinElute Cleanup Kit (Qiagen, Germantown, MD) and eluted in a final volume of 50 μL of RNA storage solution. RNA quantity was determined using a NanoDrop ND-2000 Spectrophotometer (Thermo Fisher Scientific), and RNA quality was evaluated via the RNA Integrity Number (RIN) using an Agilent 2100 Bioanalyzer (Agilent Technologies, Santa Clara, CA). All isolated RNA profiles met the strict quality thresholds (RIN>7.0) required for high-throughput transcriptomic sequencing. The comprehensive workflow encompassing these experimental and bioinformatic procedures is schematically represented in Fig. 1B.

Illumina HiSeq sequencing

The cDNA libraries were prepared using the TruSeq Stranded Total RNA Library Prep Kit (Illumina, San Diego, CA). Briefly, ribosomal RNA was removed from total RNA and the remaining RNA was purified, fragmented and primed for cDNA synthesis. First-strand cDNA was synthesized by priming the RNA fragments with random hexamers and by transcribing with reverse transcriptase. RNA template of the first strand cDNA was replaced by incorporating dUTP in place of dTTP to generate second-strand cDNA. The cDNA then underwent an end repair process, adenylation of 3' ends and subsequent ligation of the adapter. The adaptor-ligated libraries were purified and enriched with PCR to create the final cDNA library. After quality control and quantification, sequencing was performed by Psomagen Inc. (Rockville, MD) using the Illumina HiSeq 2500 platform.

***De novo* transcriptome assembly**

The raw sequence reads generated by Illumina sequencing were checked by FastQC for quality control and trimmed by Trimmomatic tool (ver. 0.32) (Bolger et al., 2014) to remove adaptors and low-quality reads. Overlapping high-quality reads were *de novo* assembled to create longer contiguous fragments (contigs) using the Trinity (version r2014-07-17) (Grabherr et al., 2011). Transcript abundance was estimated using RSEM (ver. 1.2.15) to generate FPKM (fragments per kilobase per million reads).

Functional annotation

The functional annotation of the assembled transcripts was performed using a multi-tiered pipeline incorporating Gene Ontology (GO), UniProt, the NCBI Non-Redundant protein sequences database (NR), Pfam, EggNOG, and the NCBI Nucleotide database (NT). In addition, manual annotations were conducted for those of our interest, e.g. GPCRs, based on sequence similarity searches against the NCBI NR database. These homology-based searches utilized the BLASTx algorithm with a stringent with a cut-

off E-value of 1e-5 run by Geneious 8.1.5 software (Biomatters Ltd., Auckland, New Zealand). The BLAST hits were grouped into major gene families based on their putative biological functions in slug. The organism information obtained by the BLAST hit was collected to confirm the transcript's sequence similarity to closely related species.

Differential expression analysis of tentacle transcriptome

Transcript abundance was estimated using the RNA-Seq by Expectation-Maximization (RSEM) method. Differential expression analysis was subsequently performed using the edgeR package in R (McCarthy et al., 2012). Fragments per kilobase of transcript per million mapped reads (FPKM) values were used to quantify transcript abundance and to assess tissue-specific expression patterns. Differentially expressed genes (DEGs) among PT, AT, and MT were identified through pairwise comparisons using a false discovery rate (FDR) threshold of < 0.05 and a fold-change cutoff of > 2.

Identification of chemosensory-related genes in *D. reticulatum*

The search for chemosensory-related gene sequences was based on sequence similarities to known sequences among closely related species. *De novo* transcriptome sequences of *D. reticulatum* were formatted into a local BLAST database using BioEdit (Hall, 2011). Chemosensory-related protein sequences, including G protein-coupled receptors (GPCR), ionotropic glutamate receptors (iGluR), degenerin amiloride-sensitive ion channels (DEG/ENaC), lipocalin, Niemann-Pick type C2 (NPC2), and sensory neuron membrane protein (SNMP), were retrieved from literature across diverse gastropod species (Cummins et al., 2009; Nath et al., 2025; Rondón et al., 2024). These sequences were utilized as queries in tBLASTn searches to identify homologous transcripts within the *D. reticulatum* transcriptome database.

188 **qRT-PCR**

189 Two-step qRT-PCR was performed to assess the relative abundance of transcripts for selected targets. In
190 the first step, first-strand cDNA was synthesized using the Verso cDNA synthesis kit (Thermo Fisher
191 Scientific) according to the manufacturer's protocol. Total RNAs isolated from PT, AT, and MT (See
192 Section 2.1 above for details) were used as templates for the cDNA synthesis reaction. In the second step,
193 PowerUp SYBR Green master mix for qPCR (Applied Biosystems) was used to set up the PCR reactions
194 as described in the product's manual. The qRT-PCR conditions were performed at 95 °C for 10 min; 40
195 cycles of 95 °C for 15 s and 60 °C for 1 min; followed by a melting curve analysis over the range of 60–
196 95 °C with 0.3 °C/min increments, with the specific primers (Supplementary data 5 - Table S1 and Fig.
197 S1) on StepOne Plus real-time PCR system (Applied Biosystems). Among the three housekeeping genes
198 preliminarily tested, *rpt6* (*regulatory particle triple-A ATPase 6*) was selected and used to normalize
199 signals, and relative abundance was calculated using the comparative Ct method (Supplementary Data 5 -
200 Table S2 and Fig. S2). GraphPad Prism software (Boston, MA) was used to visualize the data. One-way
201 ANOVA was run using GraphPad Prism to estimate the significance of differences in the relative
202 expression level between samples. P values < 0.05 were deemed statistically significant.

203

204 **RESULTS**

205 **Illumina sequencing, assembly and annotation**

206 A total of 228,377,020 paired-end raw reads with a GC content of 41.5% were generated. After trimming
207 the adapters and low-quality bases, a total of 227,620,062 clean reads were obtained, representing 99.7%
208 recovery of the original sequencing reads (Supplementary data 1 - Table S1). More than 60% of the clean
209 reads from each sample were mapped to produce assembled transcripts (Supplementary data 1 - Table
210 S2), resulting in a total of 142,526 transcripts with an average length of 614 bp (201 – 25,081 bp)
211 (Supplementary data 1 - Table S3). A total of 28,310 (19.9%) transcripts were annotated by at least one

method among GO, UniProt, NR, Pfam, EggNOG, NT, or manual annotation. Gene Ontology (GO) terms were assigned to the BLAST-hit contigs using Blast2Go tool, resulting in the functional annotation of 19,074 transcripts (13.4%), UniProt annotation was assigned to 17,995 transcripts (12.6%), NR resulted in the largest annotation of 27,522 transcripts (19.3%), Pfam resulted in 17,468 transcripts (12.3%), EggNOG assigned 21,073 transcripts (14.8%), NT annotated 5,266 transcripts (3.7%), and manual annotation added 179 transcripts (0.1%) (Supplementary data 1 - Table S4).

Differentially expressed genes across tentacles and mantle tissues

Global transcript distribution

To characterize the transcriptomic landscape of the slug chemosensory tissues, we evaluated the global distribution of expressed transcripts across the PT, AT, and MT for both the total unigene assembly (142,526 transcripts) (Fig. 1C) and the functionally annotated unigene subset (28,310 transcripts) (Fig. 1D).

A global comparison of the total unigene pool revealed a massive, shared core of 67,828 transcripts expressed across all three tissue types, reflecting fundamental cellular maintenance and widespread metabolic pathways. Distinct tissue-exclusive signatures were prominent across the total assembly: the mantle tissue contained the highest number of unique unigenes (19,699), followed by the posterior tentacles (8,995), while the anterior tentacles possessed the fewest tissue-specific unigenes (3,622) (Fig. 1C). Furthermore, the two tentacle pairs shared a distinct subset of 8,420 transcripts that were entirely absent in the mantle control tissue, highlighting shared candidate genes potentially dedicated to specialized tentacular or sensory functions. Within the total assembly dataset, 7,015 unigenes showed no detectable expression across the three tissue groups (Fig. 1C).

Following functional annotation, the distribution of the 28,310 annotated unigenes was separately assessed (Fig. 1D). Within this annotated subset, a core of 15,685 transcripts was shared ubiquitously

among all three tissue domains. Striking tissue-exclusive signatures persisted within the annotated dataset, demonstrating persistent functional divergence: the mantle tissue maintained the largest unique annotated signature (3,629), followed by the posterior tentacles (1,232), and the anterior tentacles (506). The PT and AT pairs shared a restricted subset of 1,150 annotated transcripts that were absent in the mantle tissue. A negligible fraction (595 transcripts) of the annotated unigenes lacked expression across these designated tissue groups (Fig. 1D).

Functional specialization of tissue-exclusive transcripts

Functional annotation of the top 30 transcripts exclusively expressed in each category highlighted the distinct physiological specialization of each tissue domain (Supplementary Data 2). The poorly characterized transcripts such as hypothetical proteins and uncharacterized proteins were excluded in these lists. **(i) Posterior tentacles (PT)-exclusive:** Transcripts restricted entirely to PT were strongly enriched in chemosensory, photoreceptive, and neural signaling components. These notably featured a prominent array of nine GPCRs—including opsins (violet-sensitive opsin-like and melanopsin-like), neuropeptide/peptide receptors (fMet-Leu-Phe, allatostatin-A, and adenosine A1-like receptors), and a chemosensory receptor—alongside neuroregulatory rho GTPase-activating proteins (RhoGAP 35 and 15), motor proteins (kinesin-like protein KIF22), solute transporters (sodium-dependent phosphate and monocarboxylate transporters), a cyclic nucleotide-gated cation channel (CNGA/B family), and synaptic vesicle-associated components (synergin γ-like) (Supplementary Data 2 - Table S1). **(ii) Anterior tentacles (AT)-exclusive:** Transcripts restricted entirely to the AT prominently featured elements involved in structural remodeling, neuroendocrine signaling, and synaptic transmission. These included extracellular matrix components (collagen α-3(VI) and cell wall protein DAN4-like), proteases (transmembrane protease serine 9-like and endothelin-converting enzyme 1), cholinergic signaling machinery—comprising acetylcholinesterase-like (AChE), nicotinic acetylcholine receptor subunit type A (nAChR), and muscarinic acetylcholine receptor M4-like—alongside multiple GPCRs (growth hormone

secretagogue receptor type 1-like and allatostatin-A receptor-like), a Cys-loop ligand-gated ion channel, and membrane transporters (sialin-like anion transporter and organic cation transporter) (Supplementary Data 2 - Table S2). **(iii) Mantle Tissue (MT)-exclusive:** Distinct from both tentacle types, the MT-exclusive profile was heavily dominated by muscular contraction and mucosal/immune defense machinery. This domain was characterized by striated muscle-specific myosin essential light chains and myosin heavy chains, alongside gastropod antimicrobial peptides (Incilarin A, B, and C), C1q domain-containing immunity factors, and a mucin-5AC-like transcript. Additionally, the MT profile featured key physiological regulators, including voltage-gated sodium channel β subunit 4, solute/ion transporters, and extracellular matrix components such as fibulin-1-like and matrilin-like 85 kDa protein (Supplementary Data 2 - Table S3).

Differential expressions within intersecting tissue categories

Comparative differential expression analysis of the overlapping tissue transcriptomes provided further resolution into regional specialization: **(i) Shared tentacular transcriptome (1,150 transcripts):** Within the pool shared exclusively between the two tentacle pairs (PT and AT), the top 30 transcripts showing higher relative expression in the PT were enriched in chemosensory, neuroendocrine, and metabolic machinery. These notably included six GPCRs—dominated by neuropeptide receptors, including four allatostatin-A receptors, a neuropeptides CAPA receptor, a thyrotropin-releasing hormone receptor, and a growth hormone secretagogue receptor—alongside five cytochrome P450 enzymes, two amiloride-sensitive sodium channel subunits (DEG/ENaC α-like and β-2-like), two tyramine β-hydroxylase transcripts, and solute/ammonium transporters (Supplementary Data 2 - Table S4). Conversely, the top 30 transcripts showing higher relative expression in the AT than the PT were heavily dominated by developmental markers, structural components, and distinct signaling pathways. The most prominently upregulated candidates included prestalk protein ($|FC|>8,000$) and basal-superficial marker (Bsmp) protein, alongside collagen α-3 (VI), trypsin-7-like protease, and a mitogen-activated protein kinase

kinase kinase (MAP3K ANP1-like). Notably, this subset also featured six GPCRs—comprising an allatostatin-A receptor-like, α-2C adrenergic receptor-like, GPCR 54-like, growth hormone secretagogue receptor type 1-like, adenosine A1-like receptor, and rhodopsin-like—as well as a cytochrome P450 enzyme (CYP2U1-like) and innexin gap junction channels (Supplementary Data 2 - Table S5). **(ii) Shared PT and MT transcriptome (4,335 transcripts):** Among the transcripts shared between PT and MT, the top 30 genes showing higher relative expression in the PT were primarily represented by neuroendocrine signaling machinery and GPCR pathways. Prominent annotated candidates included three GPCRs (adenosine receptor A1-like and two frizzled-5-like receptors), neuropeptide/peptide hormones (myomodulin 3 and insulin 4), G protein signaling regulators (regulator of G-protein signaling 3, guanine nucleotide-binding protein G(q) subunit α, and G protein-coupled receptor kinase 5), and an ABC transporter (subfamily A member 2-like) (Supplementary Data 2 - Table S6). **(iii) Shared AT and MT transcriptome (998 transcripts):** For genes shared between the AT and MT tissues, the top 30 transcripts displaying significantly higher relative expression in the AT were led bypass of stop codon protein 1 (|FC|=813.3) and prestalk protein (|FC|=369.3). Functional annotations featured key protective, metabolic, and signaling elements, including a lipocalin (fatty acid-binding protein), glutathione S-transferase 1 (GST1), trypsin-1-like, acetylcholinesterase-like (AChE), endothelin-converting enzyme 1, a single GPCR (mth2-like), and two nuclear receptors (HR3 and NR2E1) (Supplementary Data 2 - Table S7). **(iv) Ubiquitous core transcriptome (15,685 transcripts):** Finally, among the core set of transcripts expressed across all three tissue types, the top 30 transcripts showing higher expression in the PT relative to the AT were represented by candidate genes involved in metabolic processing, neuroendocrine signaling, and cell communication. These notably included three cytochrome P450 enzymes (CYP2J1-like and CYP2E1-like), two proteases (cathepsin L1-like), two GPCRs (metabotropic glutamate receptor 2 and orexin receptor type 2), an ABC transporter (subfamily G member 2-like), a neuropeptide (FMRFamide), an innexin gap junction channel (innexin unc-9-like), and cadherin cell adhesion molecules (Supplementary Data 2 - Table S8). In contrast, those with higher expression in the AT relative to the PT were predominantly composed of catalytic and structural proteins. These were heavily

dominated by various enzymes—including four chitinases, three proteases, four peptidyl-prolyl *cis-trans* isomerases, an acetylcholinesterase-like enzyme, and a single glutathione S-transferase (GST7)—alongside structural and extracellular matrix elements, such as two cell wall protein DAN4-like transcripts, matrilin-2-like, and collagen α-3(VI) (Supplementary Data 2 - Table S9).

Identification of chemosensory-related genes

To evaluate the molecular machinery underlying chemoreception in *D. reticulatum*, we specifically investigated the distribution of 1,286 annotated chemosensory-related genes across the different Venn diagram intersection categories (Table 1). These targeted families included G protein-coupled receptors (GPCRs), ionotropic glutamate receptors (iGluRs), degenerin/amiloride-sensitive sodium channels (DEG/ENaCs), lipocalins, Niemann-Pick type C2 proteins (NPC2), and sensory neuron membrane proteins (SNMPs). Overall, chemosensory candidate genes demonstrated distinct spatial partitioning, reinforcing the functional divergence between the specialized sensory tentacles and the somatic mantle tissue.

GPCR gene family

The GPCR gene family emerged as overwhelmingly dominant across almost all tissue categories, accounting for 1,193 of the 1,289 total chemosensory-related transcripts (92.7%) (Table 1). Strikingly, the highest concentration of GPCR genes was identified in the shared tentacular transcriptome (PT & AT), yielding 402 total GPCR genes. This prominent overlap underscores a substantial shared sensory receptor repertoire unique to tentacular functions. Among tissue-exclusive profiles, the posterior tentacles (PT only) maintained a substantially higher commitment to unique GPCR transcripts (264) compared to the anterior tentacles (AT only; 73), supporting a more specialized or diverse chemosensory role for the upper tentacle pair. In contrast, while the mantle tissue possessed a large number of total annotated transcripts

(3,629), only 108 of them were classified as GPCRs (Table 1), further demonstrating that these receptors are highly enriched within the sensory tentacular structures rather than somatic mantle tissues.

To systematically isolate high-confidence, chemosensory-related candidates from the total pool of 1,193 annotated GPCR transcripts, we implemented a sequential filtering workflow based on transcript localization and differential abundance (Fig. 2). Candidate GPCRs from these intersecting categories were subsequently shortlisted using stringent downstream fold change (FC) filters to capture tissue-specific enrichment. From the 264 GPCR transcripts exclusively expressed in the PT, a subset of 35 GPCR genes met the criteria for robust transcript abundance with an FPKM>2, isolating high-confidence, PT-specific sensory candidates (Fig. 2). Likewise, a subset of 9 GPCR genes was shortlisted as exclusively and robustly expressed in the AT (Fig. 2).

For transcripts shared between the two pairs of tentacles, comparative differential expression analysis partitioned candidates by regional preference. From the pool of 402 shared tentacular GPCRs (Table 1), 14 GPCRs were identified as significantly enriched in PT (|FC|>2), whereas 10 GPCRs were found to be significantly enriched in AT (|FC|>2), compared to each other (Fig. 2). Similarly, 3 and 5 GPCRs were identified as enriched in PT and AT, respectively, compared to MT. Finally, filtering the universally shared core of 178 GPCRs revealed explicit localized elevations despite broad tissue distribution. Specifically, 15 GPCRs were enriched in PT (PT>AT; |FC|>2) among those higher than MT, while 14 GPCRs were enriched in AT (AT>PT; |FC|>2).

Together, this multi-step curation pipeline successfully narrowed the broad transcriptomic dataset down to discrete sets of putative chemosensory GPCRs highly enriched in PT (a total of 67 candidate GPCRs) and in AT (a total of 38 candidate GPCRs), providing a targeted framework for subsequent functional characterization (Fig. 2). Although the 65 GPCRs were found to be MT-enriched, they were excluded from further investigation as they fell outside the sensory scope of this study. The comprehensive profiles of these shortlisted tentacle-enriched candidate GPCRs and their transcript sequences are documented in Supplementary data 3.

Non-GPCR gene families

Among the non-GPCR chemosensory gene families, distinct localized patterns were observed that suggest specialized physiological and structural roles. A total of 94 non-GPCR chemosensory candidate transcripts were identified as differentially expressed across the three tissue types, comprising 40 ionotropic glutamate receptors (iGluRs), 34 degenerin/amiloride-sensitive sodium channels (DEG/ENaCs), 12 lipocalins, 3 Niemann-Pick type C2 proteins (NPC2), and 4 sensory neuron membrane proteins (SNMPs) (Table 1).

(A) iGluRs

The 40 identified iGluRs displayed a high abundance in the mantle tissue and mixed-tissue profiles, while only three iGluRs showed tentacle-specific expression with 2 in PT and 1 in AT (Fig. 3A). A majority of iGluR transcripts were localized within the shared core across all three tissues (12 iGluRs) and exclusively within the mantle tissue only (12 iGluRs). Additionally, 9 iGluRs were expressed in both the PT and MT, while 4 iGluRs were found in the AT and MT comparison (Fig. 3A). This distinct leaning toward mantle-containing profiles suggests that iGluRs may coordinate pervasive somatic sensory networks or peripheral chemical feedback systems in the slug body wall. Intriguingly, among the tentacle-specific transcripts restricted exclusively to distinct tentacular types, c123747_g1_i1 (*glutamate receptor subunit protein GluR7 precursor*) was selectively expressed in PT only, whereas c88995_g1_i1 (*glutamate receptor ionotropic, kainate 4-like*) was unique to AT only (Supplementary Data 4 – Table S1). Among those expressed in multiple tissues, c96868_g1_i1 and c88280_g1_i1 were higher in PT and AT, respectively. Taken together, this analysis indicates that iGluRs play a minor but highly specialized roles in divergent tentacular sensing.

(B) DEG/ENaC channels

The DEG/ENaC ion channel family (34 transcripts total) was broadly distributed throughout the target tissues but demonstrated substantial localized enrichment within the core ubiquitous transcriptome (12 transcripts) and mantle tissue (9 transcripts) profiles, implying substantial involvement in non-tentacular tactile reception or localized somatic monitoring (Fig. 3B). However, highly localized sensory markers were also present; c80151_g1_i1 (*amiloride-sensitive sodium channel subunit alpha-like*), c84991_g3_i2 (*subunit beta-2-like*), c74351_g1_i1 (*amiloride-sensitive sodium channel subunit alpha-like*), and c74351_g2_i1 (*acid-sensing ion channel 1-like*) were heavily enriched in PT, exhibiting prominent upregulated expressions in the PT compared to the AT; while c133010_g1_i1 (*amiloride-sensitive sodium channel subunit beta-like*), c123636_g1_i1 (*acid-sensing ion channel 1-like*), and c100848_g1_i1 (*amiloride-sensitive sodium channel subunit beta-like*) were higher in AT than PT, exhibiting prominent upregulated expressions in the AT compared to the PT (Supplementary Data 4 – Table S2).

(C) Lipocalin, NPC2, and SNMP

The auxiliary transport and binding protein families, lipocalins (12 total), NPC2s (3 total), and SNMPs (4 total), were primarily restricted to interconnected tissue profiles (Fig. 3C-3E). Both lipocalins and NPC2 expressions were entirely absent from tissue-exclusive categories (PT only, AT only, or MT only). Instead, lipocalins and NPC2s were predominantly localized within the ubiquitous core shared by all three tissues (9 lipocalins and 3 NPC2s), highlighting their fundamental roles in systemic hydrophobic ligand binding or general transport (Fig. 3C & 3D). The remaining lipocalins were found in shared tentacle-mantle niches (2 in PT & MT, 1 in AT & MT) (Fig. 3C). By the fold change analysis of lipocalins, c78360_g1_i1 (*fatty acid-binding protein, muscle-like*) was higher in both PT and AT, compared to MT, while c76900_g1_i1 (*fatty acid-binding protein*) was almost exclusively high in AT (Supplementary Data 4 – Table S3). In contrast, SNMPs were explicitly absent from the universally shared core, appearing exclusively in the mantle tissue (1 transcript) or within shared tentacle-mantle coordinates (2 in PT & MT, 1 in AT & MT) (Fig. 3E), revealing no particular tentacle-enriched NPC2 or SNMPs (Supplementary Data 5 – Tables S4-S5). Taken together, these distribution profiles indicate an intricate

tissue-specific sorting of non-GPCR candidate chemosensory elements, including a majority of mantle-enriched ion channels and systemic transport proteins, balanced with a minor numbers of tentacle-enriched ones.

qRT-PCR validation of selected GPCR transcripts

To validate the tissue-specific expression profiles obtained from the RNA-Seq analysis, a total of 17 candidate GPCR genes were selected for quantitative real-time PCR (qRT-PCR) analysis. These genes were chosen based on their distinctive transcript abundance patterns across the tissues: 5 were predominantly expressed in the posterior tentacles (PT), 7 showed high expression in both the posterior and anterior tentacles (PT & AT), and 5 were preferentially expressed in the anterior tentacles (AT) (Table 2). Among three candidate internal reference genes evaluated in preliminary optimization trials, the *rpt6* gene was selected for target gene normalization due to its superior expression stability across all tested tissue types (Supplementary Data 5 - Table S2 and Fig. S1). The PT tissue served as the baseline control (set as 1.0) for all relative expression calculations. Relative transcript abundance was calculated from three technical replicates per biological sample, with standard deviations represented as error bars (Fig. 4).

The qRT-PCR expression profiles largely mirrored the relative abundance trends observed in the *in silico* RNA-Seq dataset; 14 of the 17 tested transcripts exhibited the anticipated enrichment in the PT. The remaining three targets displayed alternative patterns that varied slightly from the RNA-Seq predictions: c69183_g1_i1 was confirmed to be highly abundant in the AT, while c89048_g1_i1 and c106522_g1_i1 demonstrated elevated expression across both tentacle types (PT & AT) relative to MT (Fig. 3). Taken together, these validated, tissue-specific profiles indicate that these candidate genes represent high-priority targets for downstream functional characterization. Detailed data regarding the qRT-PCR assays are provided in Supplementary Data 5.

DISCUSSION

The chemosensory system is essential for survival, foraging, predator avoidance, and reproductive success in terrestrial snails and slugs (Kiss, 2017). At the molecular level, detecting chemical signals relies on specialized proteins belonging to medium- to large-sized multigene families present across taxa in the animal kingdom (Nei et al., 2008). Although terrestrial gastropods are known to navigate complex environments using airborne and substrate-borne chemical cues, the molecular mechanisms underlying these behaviors remain poorly understood.

This study provides a comprehensive transcriptomic resource for one of the world's most damaging slug pests, *Deroceras reticulatum*, with a specific focus on its primary sensory structures: the posterior (PT) and anterior (AT) tentacles. Prior to this work, publicly available sequence resources for *D. reticulatum* in NCBI (PRJNA384817 and PRJNA167149) were limited in their representation of the chemosensory gene repertoire because they were derived from whole-body transcriptomes. Building upon our previous whole-body identification of slug neuropeptide repertoires (Ahn et al., 2017), our de novo assembly generated 142,526 unigenes with an average length of 614 bp. Although our overall structural annotation rate (19.9% of total transcripts annotated) reflects the typical limitations of working with non-model gastropod genomes, the absolute number of fully annotated transcripts (28,310) represents a high-resolution dataset vital for exploring terrestrial slug physiology. Nonetheless, the substantial fraction of unannotated unigenes highlights a vast molecular diversity requiring further functional characterization.

The presence of two pairs of tentacles is a defining morphological characteristic of the terrestrial pulmonate order Stylommatophora, distinguishing them from aquatic Basommatophora, which possess only a single pair (Croll, 1983). Molecular phylogenetic and microanatomical analyses suggest that this dual-tentacle system evolved by the splitting of an original single ancestral pair as an adaptation to life on land (Brenzinger et al., 2021). Our comparative transcriptomic data strongly reinforce this evolutionary

split, showing an underlying core of shared sensory transcripts paired with a robust transcriptomic divergence between the individual tentacle pairs.

Pairwise differential expression analysis and functional annotations further illuminate the distinct physiological specialization between the two tentacle pairs. Behavioral studies have shown that the lower, anterior tentacles are positioned close to the ground for substrate contact chemoreception and trail-following, whereas the upper, posterior tentacles project upward to specialize in airborne olfaction and wind orientation (Ito et al., 2000; Kiss, 2017). This functional divergence is clearly reflected in our data: the PT transcriptome is strongly associated with long-range neurosensory functions, as indicated by the abundance of neural pathways, photoreception cascades (supporting the apical optical spot), and expansive chemosensory receptor repertoires. In contrast, the AT transcriptome appears adapted for localized mechanical interaction and chemical processing, enriched with structural remodeling proteins, extracellular proteases, and synaptic transmission machinery. By demonstrating that the PT manages aerial olfaction and vision while the AT is linked to tactile and contact chemoreception, our findings underscore how the dual-tentacle configuration serves as a key sensory innovation enabling stylommatophoran slugs to successfully navigate and live in complex terrestrial habitats.

Among the candidate chemosensory gene families identified in gastropods, GPCRs represent the predominant group, matching trends observed in the sea hare *A. californica* (Cummins et al., 2009a), the golden apple snail *Pomacea canaliculata* (Rondón et al., 2024), and the Mediterranean cone snail *Lautoconus ventricosus* (Rondón et al., 2024). In *D. reticulatum*, GPCRs accounted for 1,193 of the 1,289 total annotated chemosensory-related transcripts (92.7%), with Class A rhodopsin-like receptors comprising the vast majority (Table 1). Our multi-step filtration pipeline successfully narrowed this extensive repertoire down to high-confidence sensory candidates based on tissue-specific localization and abundance thresholds.

The large number of GPCRs identified from the *D. reticulatum* tentacular transcriptome suggests lineage-specific gene duplications. Although formal phylogenetic analysis remains to be performed to precisely

map these duplication events in *D. reticulatum*, similar expansions of the Class A GPCR family have been documented in *A. californica* and other Mollusca, and are thought to reflect evolutionary adaptations to shifting chemical landscapes (Nath et al., 2025). A terrestrial slug, navigating a multi-dimensional chemical landscape containing for example volatile plant defense compounds, odors of plant and animal decomposition, soil microclimate indicators, and specialized mucus pheromones and kairomones, requires a highly adaptable and diverse receptor repertoire (Wang et al., 2026). Consequently, investigating these lineage-specific duplications through dedicated phylogenetic and syntenic analyses would represent a crucial next step to clarify the evolutionary trajectory of gastropod chemoreceptors. Moreover, because many tentacle-enriched candidates remain orphan receptors with unknown ligands, systematic curation of these localized networks provides a strategic roadmap for downstream deorphanization studies (Ahn et al., 2020). Such studies will be essential for uncovering the molecular, structural, and evolutionary basis of chemosensation in terrestrial slugs.

Although GPCRs remain the primary focus of chemosensory research, our findings indicate that slug peripheral sensation relies on a multi-tiered network of ion channels and auxiliary transport proteins. The localized expression of specific ionotropic glutamate receptors (iGluRs) and variant ionotropic receptors (IRs) in the PT and AT suggests the presence of an ancient and conserved olfactory mechanism. In insects and aquatic mollusks, IR networks act as precise, rapid detectors for volatile amines and acids (Benton et al., 2009; Croset et al., 2010; Liang et al., 2016; Wang et al., 2026; Yamagishi et al., 2008). The identification of distinct, mutually exclusive iGluR/IR variants within individual tentacle types suggests that *D. reticulatum* utilizes parallel ionotropic pathways to separate different classes of chemical inputs.

Similarly, the differential distribution of the DEG/ENaC ion channel family indicates a highly organized sensory interface. Members of this superfamily function as non-voltage-gated mechanoreceptors, acid-sensing ion channels, or salt taste receptors (Bianchi and Driscoll, 2002; Kaulich et al., 2023; Mano and Driscoll, 1999). While widespread somatic expression across the mantle tissue suggest a role in general neuromuscular coordination, the distinct enrichment of specific DEG/ENaC variants within either the PT

or AT points to targeted sensory tasks. These channels likely allow the slug to integrate mechanical feedback (such as substrate texture or wind speed) with localized chemical cues, facilitating a multimodal assessment of its surroundings.

Finally, our data clarify how terrestrial gastropods overcome the biophysical challenge associated with detecting airborne chemical cues. Hydrophobic odorants must be captured and transferred across the hydrophilic mucus layer overlaying the sensory dendrites (Zarzo, 2007). In insects, this function is carryout by specialized odorant-binding proteins (OBPs) (Pelosi et al., 2005). Although classical insect OBPs appear to be evolutionarily absent in Mollusca (Rihani et al., 2021), our analysis identified potential functional analogs, including secreted Niemann-Pick type C2 (NPC2) proteins (Storch and Xu, 2009) and specialized lipocalins (Zhu et al., 2021). These extracellular carriers likely act as solubilizing chaperones within the tentacular mucus, capturing hydrophobic environmental lipid cues and delivering them to nearby chemoreceptors. This highlights a compelling example of functional convergence in terrestrial chemoreception.

In addition to its evolutionary insights, the tissue-specific receptor blueprint developed in this study provides a valuable resource for applied agricultural biotechnology. *D. reticulatum* is a globally important agricultural pest that causes extensive damage to a diverse range of crops (Howlett, 2012; Port and Port, 1989). Current management strategies rely heavily on broad-spectrum chemical molluscicide baits, which are often limited by variable efficacy, rapid degradation under wet conditions, and toxicity to non-target organisms (Dively and Patton, 2022; Mustapha et al., 2025). There is thus an urgent need to develop new control tactics for this and other terrestrial gastropod pest species.

Because peripheral GPCRs and ion channels are directly exposed to the external environment, they represent promising targets for highly selective, next-generation behavioral disruptors and species-specific molluscicides. The high-confidence, tentacle-enriched candidates validated by our qRT-PCR pipeline provide concrete targets for high-throughput chemical screening and for the design of sequence-specific double-stranded RNAs (dsRNAs) for targeted RNA interference (RNAi) applications. By

identifying the specific molecular components that govern slug orientation and foraging behaviors, these transcriptomic profiles establish a foundation for innovative, biorational management strategies designed to disrupt chemosensory-mediated communication and protect vulnerable agroecosystems.

Acknowledgements

We thank Nivetha Ramanathan for preparing aliquots of the qPCR primers.

Author Contributions

S.-J.A.: Conceptualization; Methodology; Investigation; Formal analysis; Validation; Visualization; Software; Writing – original draft; Writing – review & editing **H.S.J.:** Investigation; Methodology; Validation; Writing – original draft; Writing – review & editing **R.D.M.:** Resources; Funding acquisition; Writing – review & editing **M.-Y.C.:** Conceptualization; Methodology; Investigation; Formal analysis; Resources; Funding acquisition; Writing – review & editing; Project administration; Supervision

Funding

This work was supported in part by the Oregon Grass Seed Commissions, the Oregon Association of Nurseries, and USDA base funds (CRIS 2072-22000-040-00D) awarded to author M.C. Author R.M. also received research support from the Agricultural Experiment Station through Hatch Act capacity funding (grant number NI25HMFPXXXXG029) from the USDA National Institute of Food and Agriculture.

Data Availability

The raw RNA-Seq data generated and analyzed during the current study are deposited in the NCBI Sequence Read Archive (SRA) repository under BioProject accession number [PRJNA1527565] and SRA submission number [SUB16477613]. These datasets are currently scheduled for release upon publication of this manuscript.

Declarations

Ethics approval and consent to participate Not applicable.

Consent for publication Not applicable.

Competing interests The authors declare no competing interests.

References

Ahn, S.-J., Martin, R., Rao, S., Choi, M.-Y., 2017. Neuropeptides predicted from the transcriptome analysis of the gray garden slug *Deroceras reticulatum*. Peptides 93, 51–65. https://doi.org/10.1016/j.peptides.2017.05.005

Ahn, S.J., Mc Donnell, R.J., Corcoran, J.A., Martin, R.C., Choi, M.Y., 2020. Identification and functional characterization of the first molluscan neuromedin U receptor in the slug, *Deroceras reticulatum*. Sci. Rep. 10, 22308. https://doi.org/10.1038/s41598-020-79047-x

Arias, R.O., 1960. The biology of the grey garden slug *Deroceras reticulatum* (Müller) (Master Thesis). Oregon State College. https://agsci.oregonstate.edu/sites/agscid7/files/arias-crowell-1963-gray-slug.pdf

Barker, G.M. (2002) Molluscs as Crop Pests. CABI Publishing, Oxfordshire, United Kingdom.

Barker, G.M. (2004) Natural Enemies of Terrestrial Molluscs. CABI Publishing, Oxfordshire, United Kingdom.

Benton, R., Vannice, K.S., Gomez-Diaz, C., Vosshall, L.B., 2009. Variant ionotropic glutamate receptors as chemosensory receptors in *Drosophila*. Cell 136, 149–162. https://doi.org/10.1016/j.cell.2008.12.001

Bianchi, L., Driscoll, M., 2002. Protons at the gate: DEG/ENaC ion channels help us feel and remember. Neuron 34(3), 337–340. https://doi.org/10.1016/S0896-6273(02)00687-6

Bolger, A.M., Lohse, M., Usadel, B., 2014. Trimmomatic: a flexible trimmer for Illumina sequence data. Bioinformatics 30, 2114–2120. https://doi.org/10.1093/bioinformatics/btu170

Brenzinger, B., Schrödl, M., Kano, Y., 2021. Origin and significance of two pairs of head tentacles in the radiation of euthyneuran sea slugs and land snails. Sci. Rep. 11, 21016. https://doi.org/10.1038/s41598-021-99172-5

Brody, T., Cravchik, A., 2000. *Drosophila melanogaster* G protein–coupled receptors. J Cell Biol.150, 83–88. https://doi.org/10.1083/jcb.150.2.F83

CABI, 2022. *Deroceras reticulatum* (grey field slug). CABI Compendium. https://doi.org/10.1079/cabicompendium.85752

Chase, R., 1986. Lessons from snail tentacles. Chem. Senses 11, 411–426. https://doi.org/10.1093/chemse/11.4.411

Chase, R., Croll, R.P., 1981. Tentacular function in snail olfactory orientation. J. Comp. Physiol. A Neuroethol. Sens. Neural Behav. Physiol. 143, 357–362. https://doi.org/10.1007/BF00611173

Chase, R., Tolloczko, B., 1993. Tracing neural pathways in snail olfaction: From the tip of the tentacles to the brain and beyond. Microsc. Res. Tech. 24, 214–230. https://doi.org/10.1002/jemt.1070240303

Choi, M.-Y., Price, B., Hafeez, M., Martin, R., Richart, C., Donnell, R.M., 2024. Bioactive peptides inhibit feeding activity in the grey garden slug, *Deroceras reticulatum*. Pest Manag. Sci. 80, 6493–6500. https://doi.org/10.1002/ps.8386

Croll, R.P., 1983. Gastropod chemoreception. Biological Reviews 58, 293–319. https://doi.org/10.1111/j.1469-185x.1983.tb00391.x

Croset, V., Rytz, R., Cummins, S.F., Budd, A., Brawand, D., Kaessmann, H., Gibson, T.J., Benton, R., 2010. Ancient protostome origin of chemosensory ionotropic glutamate receptors and the evolution of insect taste and olfaction. PLoS Genet. 6, e1001064. https://doi.org/10.1371/journal.pgen.1001064

Cummins, S.F., Erpenbeck, D., Zou, Z., Claudianos, C., Moroz, L.L., Nagle, G.T., Degnan, B.M., 2009a. Candidate chemoreceptor subfamilies differentially expressed in the chemosensory organs of the mollusc *Aplysia*. BMC Biol. 7, 28. https://doi.org/10.1186/1741-7007-7-28

Cummins, S.F., Leblanc, L., Degnan, B.M., Nagle, G.T., 2009b. Molecular identification of candidate chemoreceptor genes and signal transduction components in the sensory epithelium of *Aplysia*. Journal of Experimental Biology 212, 2037–2044. https://doi.org/10.1242/jeb.026427

Dively, G.P., Patton, T., 2022. An evaluation of cultural and chemical control practices to reduce slug damage in no-till corn. Insects 13(3), 277. https://doi.org/10.3390/insects13030277

Frain, J.M., 1980. Chemoreception and feeding in the grey field slug, *Deroceras reticulatum* (Müller), with reference to molluscicide formulation. Westfield College, London University.

Fredriksson, R., Lagerström, M.C., Lundin, L.-G., Schiöth, H.B., 2003. The G-protein-coupled receptors in the human genome form five main families. Phylogenetic analysis, paralogon groups, and fingerprints. Mol. Pharmacol. 63, 1256–1272. https://doi.org/https://doi.org/10.1124/mol.63.6.1256

Glen, D.M. and Symondson, W.O.C. (2003) Influence of Soil Tillage on Slugs and Their Natural Enemies. In: Soil Tillage in Agroecosystems (Ed. El Titi, A.), CRC Press LLC, pp. 207-227.

Godan, D., 1983. Pest slugs and snails - Biology and control. Springer-Verlag, Berlin.

Grabherr, M.G., Haas, B.J., Yassour, M., Levin, J.Z., Thompson, D.A., Amit, I., Adiconis, X., Fan, L., Raychowdhury, R., Zeng, Q., Chen, Z., Mauceli, E., Hacohen, N., Gnirke, A., Rhind, N., Di Palma, F., Birren, B.W., Nusbaum, C., Lindblad-Toh, K., Friedman, N., Regev, A., 2011. Full-length transcriptome assembly from RNA-Seq data without a reference genome. Nat. Biotechnol. 29, 644–652. https://doi.org/10.1038/nbt.1883

Hafeez, M., Mc Donnell, R., Colton, A., Howe, D., Denver, D., Martin, R.C., Choi, M.Y., 2024. Immune-related gene profiles and differential expression in the grey garden slug *Deroceras reticulatum* infected with the parasitic nematode *Phasmarhabditis hermaphrodita*. Insects 15, 311. https://doi.org/10.3390/insects15050311

Hall, T.A., 2011. BioEdit: An important software for molecular biology. GERF Bulletin of Biosciences 2(1), 60–61.

Hanlon, C.D., Andrew, D.J., 2015. Outside-in signaling - A brief review of GPCR signaling with a focus on the *Drosophila* GPCR family. J. Cell Sci. 128, 3533–3542. https://doi.org/10.1242/jcs.175158

Harty, B.L., Krishnan, A., Sanchez, N.E., Schiöth, H.B., Monk, K.R., 2015. Defining the gene repertoire and spatiotemporal expression profiles of adhesion G protein-coupled receptors in zebrafish. BMC Genomics 16. https://doi.org/10.1186/s12864-015-1296-8

Howlett, S.A., 2012. Terrestrial slug problems: classical biological control and beyond. CABI Reviews 1–10. https://doi.org/10.1079/PAVSNNR20127051

Howlett, S.A., 2005. The biology, behaviour and control of the field slug *Deroceras reticulatum* (Müller) (PhD Thesis). Newcastle University. https://theses.ncl.ac.uk/jspui/handle/10443/1640

Iglesias, J., Castillejo, J., Ester, A., 2002. Laboratory evaluation of potential molluscicides for the control of eggs of the pest slug *Deroceras reticulatum* (Müller) (Pulmonata: Limacidae). Int. J. Pest Manag. 48, 19–23. https://doi.org/10.1080/09670870110062553

Ito, I., Nakamura, H., Kimura, T., Suzuki, H., Sekiguchi, T., Kawabata, K., Ito, E., 2000. Neuronal components of the superior and inferior tentacles in the terrestrial slug, *Limax marginatus*. Neuroscience Research 37(3), 191-200. https://doi.org/10.1016/S0168-0102(00)00118-8

Kaulich, E., Grundy, L.J., Schafer, W.R., Walker, D.S., 2023. The diverse functions of the DEG/ENaC family: linking genetic and physiological insights. J. Physiol. 601, 1521–1542. https://doi.org/10.1113/JP283335

Kiss, T., 2017. Do terrestrial gastropods use olfactory cues to locate and select food actively? Invertebrate Neuroscience 17, 9. https://doi.org/10.1007/s10158-017-0202-2

Krishnan, A., Schiöth, H.B., 2015. The role of G protein-coupled receptors in the early evolution of neurotransmission and the nervous system. Journal of Experimental Biology 218 (4): 562–571. https://doi.org/10.1242/jeb.110312

Liang, D., Wang, T., Rotgans, B.A., McManus, D.P., Cummins, S.F., 2016. Ionotropic receptors identified within the tentacle of the freshwater snail *Biomphalaria glabrata*, an intermediate host of *Schistosoma mansoni*. PLoS One 11, e0156380. https://doi.org/10.1371/journal.pone.0156380

Lovett, A.L., Black, A.B., 1920. The gray garden slug with notes on allied forms. Oregon Agricultural College Experiment Station Bulletin 170, 83–97. https://agsci.oregonstate.edu/sites/agscid7/files/arias-crowell-1963-gray-slug.pdf

Mano, I., Driscoll, M., 1999. DEG/ENaC channels: A touchy superfamily that watches its salt. BioEssays 21(7), 568-578. https://doi.org/10.1002/(SICI)1521-1878(199907)21:7<568::AID-BIES5>3.0.CO;2-L

McCarthy, D.J., Chen, Y., Smyth, G.K., 2012. Differential expression analysis of multifactor RNA-Seq experiments with respect to biological variation. Nucleic Acids Res. 40, 4288–4297. https://doi.org/10.1093/nar/gks042

Mc Donnell, R.J., Vendetti, J., Paine, T.D. and Gormally, M.J. (2024) Slugs: A Guide to the Invasive and Native Fauna of California. 2nd Edition. University of California Agricultural and Natural Resources Publications (37 pp.). https:/ /doi.org/10.3733/UZUM1090 anrpublications.org.

Mombaerts, P., 1999. Seven-transmembrane proteins as odorant and chemosensory receptors. Science 286, 707–711. https://doi.org/10.1126/science.286.5440.70

Morishita, F., 2017. Neuropeptides and their physiological functions in mollusks, in: Horiguchi, T. (Ed.), Biological Effects by Organotins. Springer Japan, Tokyo, pp. 167–197. https://doi.org/10.1007/978-4-431-56451-5_8

Mustapha, S., Loveridge, E.J., Butt, T.M., Vuts, J., Ortega-Ramos, P.A., Cook, S.M., 2025. Semiochemical applications for managing the grey field slug (*Deroceras reticulatum* Müller), a major pest of arable crops. Pest Manag. Sci. 81(11), 7288-7301. https://doi.org/10.1002/ps.70007

Nath, R., Panda, B., Rakesh, S., Krishnan, A., 2025. Lineage-specific Class-A GPCR dynamics reflect diverse chemosensory adaptations in Lophotrochozoa. Mol. Biol. Evol. 42, msaf042. https://doi.org/10.1093/molbev/msaf042

Nei, M., Niimura, Y., Nozawa, M., 2008. The evolution of animal chemosensory receptor gene repertoires: Roles of chance and necessity. Nat. Rev. Genet. 9, 951–963. https://doi.org/10.1038/nrg2480

Pelosi, P., Calvello, M., Ban, L., 2005. Diversity of odorant-binding proteins and chemosensory proteins in insects. Chemical Senses 30(Suppl_1), i291–i292. https://doi.org/10.1093/chemse/bjh229

Port, C.M., Port, G.R., 1989. The biology and behavior of slugs in relation to crop damage and control, in: Russell, G.E. (Ed.), Management and Control of Invertebrate Crop Pests. Intercept, Andover, Hampshire, U.K., p. 379.

Rihani, K., Ferveur, J.-F., Briand, L., 2021. The 40-year mystery of insect odorant-binding proteins. Biomolecules 11(4), 509. https://doi.org/10.3390/biom11040509

Rondón, J.J., Pisarenco, V.A., Ramón Pardos-Blas, J., Sánchez-Gracia, A., Zardoya, R., Rozas, J., 2024. Comparative genomic analysis of chemosensory-related gene families in gastropods. Mol. Phylogenet. Evol. 192, 107986. https://doi.org/10.1016/j.ympev.2023.107986

Runham, N.W., 1978. Reproduction and its control in *Deroceras reticulatum*. Malacologia 17, 341–350.

South, A., 1992. Terrestrial slugs: Biology, ecology and control. Springer Netherlands, Dordrecht. https://doi.org/10.1007/978-94-011-2380-8

Stephenson, J.W., 1979. The functioning of the sense organs associated with feeding behaviour in *Deroceras reticulatum* (Müll.). Journal of Molluscan Studies 45, 167–171. https://doi.org/10.1093/oxfordjournals.mollus.a065491

Storch, J., Xu, Z., 2009. Niemann-Pick C2 (NPC2) and intracellular cholesterol trafficking. Biochim. Biophys. Acta Mol. Cell Biol. Lipids 1791(7), 671-678. https://doi.org/10.1016/j.bbalip.2009.02.001

Tan, L., Grewal, P.S., 2001. Infection behavior of the Rhabditid nematode *Phasmarhabditis hermaphrodita* to the grey garden slug *Deroceras reticulatum*. J. Parasitol. 87, 1349–1354. https://doi.org/10.1645/0022-3395(2001)087[1349:IBOTRN]2.0.CO;2

Tulli, M.C., Carmona, D.M., López, A.N., Manetti, P.L., Vincini, A.M., Cendoya, G., 2009. Predation on the slug *Deroceras reticulatum* (pulmonata: Stylommatophora) by *Scarites anthracinus* (Coleoptera: Carabidae). Ecologia Austral 19, 55–61. https://www.scielo.org.ar/scielo.php?script=sci_arttext&pid=S1667-782X2009000100005

Ucciferri, C.C., Wyeth, R.C., 2023. Chemosensory afference in the tentacle nerve of *Lymnaea stagnalis*. Invertebrate Biology 142, e12414. https://doi.org/10.1111/ivb.12414

Vidal, B., Aghayeva, U., Sun, H., Wang, C., Glenwinkel, L., Bayer, E.A., Hobert, O., 2018. An atlas of *Caenorhabditis elegans* chemoreceptor expression. PLoS Biol. 16, e2004218. https://doi.org/10.1371/journal.pbio.2004218

Wang, G., Sun, Y.-Q., Wang, F., Wang, Z.-Y., Sun, N.-Y., Wei, M.-J., Shen, Y.-T., Li, Y.-J., Sun, Q.-Q., Fujaya, Y., Bian, X.-G., Yang, W.-Q., Tan, K., 2026. Genome-wide characterization of four

gastropod species ionotropic receptors reveals diet-linked evolutionary patterns of functional divergence. Animals 16, 172. https://doi.org/10.3390/ani16020172

Weis, W.I., Kobilka, B.K., 2018. The molecular basis of G protein-coupled receptor activation. Annual Review of Biochemistry 87, 897-919. https://doi.org/10.1146/annurev-biochem-060614-033910

Xu, B., Kong, L., Sun, J., Zhang, J., Zhang, Y., Song, H., Li, Q., Uribe, J.E., Halanych, K.M., Cai, C., Dong, Y.W., Wang, S., Li, Y., 2025. Molluscan systematics: Historical perspectives and the way ahead. Biological Reviews 100, 672–697. https://doi.org/10.1111/brv.13157

Yamagishi, M., Ito, E., Matsuo, R., 2008. Redundancy of olfactory sensory pathways for odor-aversion memory in the terrestrial slug *Limax valentianus*. J. Exp. Biol. 211, 1841–1849. https://doi.org/10.1242/jeb.018028

Zarzo, M., 2007. The sense of smell: Molecular basis of odorant recognition. Biological Reviews. https://doi.org/10.1111/j.1469-185X.2007.00019.x

Zhu, J., Iannucci, A., Dani, F.R., Knoll, W., Pelosi, P., 2021. Lipocalins in arthropod chemical communication. Genome Biol. Evol. 13(6), evab091. https://doi.org/10.1093/gbe/evab091

Figure legends

Figure 1. Transcriptome analysis of the *Deroceras reticulatum* tentacles. (A) Representative image of the gray field slug, *D. reticulatum*, highlighting the primary cephalic sensory and non-sensory tissues investigated: posterior tentacles (PT), anterior tentacles (AT), and mantle tissue (MT). **(B)** Schematic overview of the experimental and bioinformatic workflow, from tissue dissection and total RNA extraction, through RNA sequencing and transcriptome assembly. Downstream analysis incorporates parallel automated annotation and targeted manual annotation to identify chemosensory candidate genes for tissue-differential expression profiling. **(C)** Venn diagram showing the tissue-specific and overlapping distribution of all 142,526 assembled unigenes across PT, AT and MT. **(D)** Venn diagram showing the tissue-specific and overlapping distribution of the 28,310 annotated unigenes.

Figure 2. Filtering and identification of tentacle-enriched G protein-coupled receptors (GPCRs) from the transcriptome dataset. Candidate GPCRs were filtered through sequential analyses, including transcript annotation, transcript abundance by FPKM, and differential expression analysis by FC in the three different tissues, posterior tentacles (PT), anterior tentacles (AT), and mantle tissue (MT), resulting in the identification of putative chemosensory GPCRs enriched in tentacular tissues. Numbers within the Venn diagram indicate the number of all GPCRs expressed in the corresponding tissue categories. Numbers at the ends of the arrows outside the Venn diagram represent tissue-enriched GPCRs that met the selection criteria indicated beneath each value. The details of the MT-enriched GPCRs are not shown here. Corresponding gene lists and nucleotide sequences are provided in Supplementary Data 3.

Figure 3. Tissue distribution of non-GPCR chemosensory candidate gene families in *Deroceras reticulatum*. Venn diagrams illustrate overlapping and tissue-exclusive transcripts across posterior tentacle, anterior tentacle, and mantle transcriptomes. **(A)** Ionotropic glutamate receptors (iGluRs) predominantly distributed in ubiquitous and mantle-containing profiles. **(B)** Degenerin/amiloride-sensitive sodium channels (DEG/ENaCs) distributed broadly across all domains. **(C)** Lipocalins and **(D)** Niemann-Pick type C2 proteins (NPC2) concentrated entirely within the shared universal core. **(E)** Sensory neuron membrane proteins (SNMPs) restricted to mantle-containing coordinates and absent from the shared core. Corresponding gene lists and nucleotide sequences are provided in Supplementary Data 4.

Figure 4. Relative expression levels of selected GPCR genes in the three tissues of *Deroceras reticulatum*. The relative expression levels of 17 candidate G protein-coupled receptor (GPCR) transcripts and three reference genes (*rpt6*, *rpl3*, and *rpl40*) were evaluated by qRT-PCR in posterior tentacles (PT), anterior tentacles (AT), and mantle tissue (MT). Candidate transcripts were selected based on tissue-specific expression patterns identified by RNA sequencing. Differentially expressed genes and

control genes identified by RNA-seq were evaluated for relative abundance using qRT-PCR. These empirical evaluations revealed that 14 GPCR genes are highly expressed in PT, compared to AT and MT, while one GPCR (c69183_g1_i1) is exclusively highly expressed AT and two GPCRs (c89048_g1_i1 and c106522_g1_i1) are equally expressed in both PT and AT. Signal was normalized using *rpt6*. Means of three technical replicates are shown with standard-deviation error bars. Statistically significant differences are marked by different letters ($p < 0.05$), as determined by Tukey's HSD multiple comparisons test.

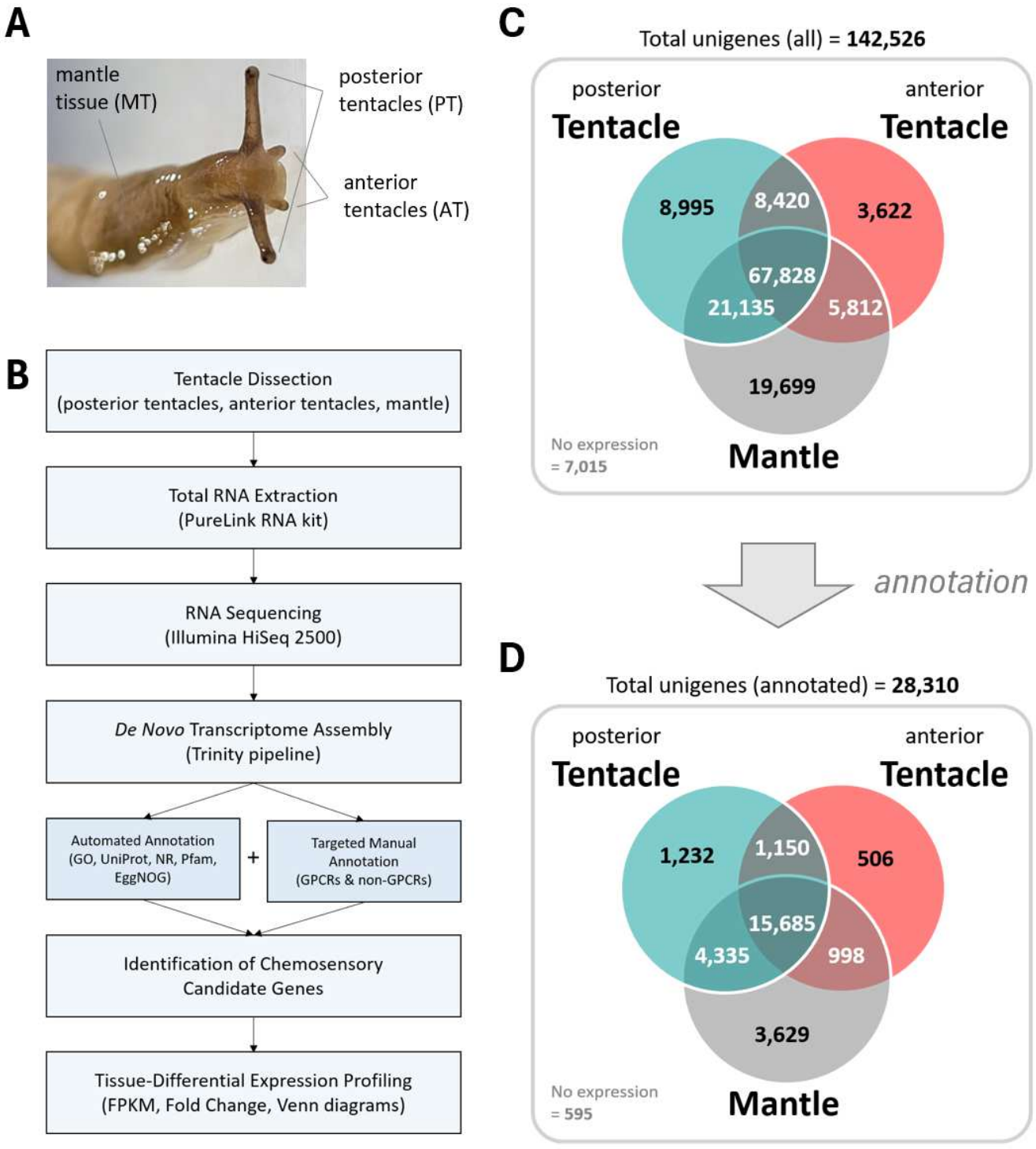


Figure 1. Transcriptome analysis of the *Deroceras reticulatum* tentacles. (A) Representative image of the gray field slug, *D. reticulatum*, highlighting the primary cephalic sensory and non-sensory tissues investigated: posterior tentacles (PT), anterior tentacles (AT), and mantle tissue (MT). **(B)** Schematic overview of the experimental and bioinformatic workflow, from tissue dissection and total RNA extraction, through RNA sequencing and transcriptome assembly. Downstream analysis incorporates parallel automated annotation and targeted manual annotation to identify chemosensory candidate genes for tissue-differential expression profiling. **(C)** Venn diagram showing the tissue-specific and overlapping distribution of all 142,526 assembled unigenes across PT, AT and MT. **(D)** Venn diagram showing the tissue-specific and overlapping distribution of the 28,310 annotated unigenes.

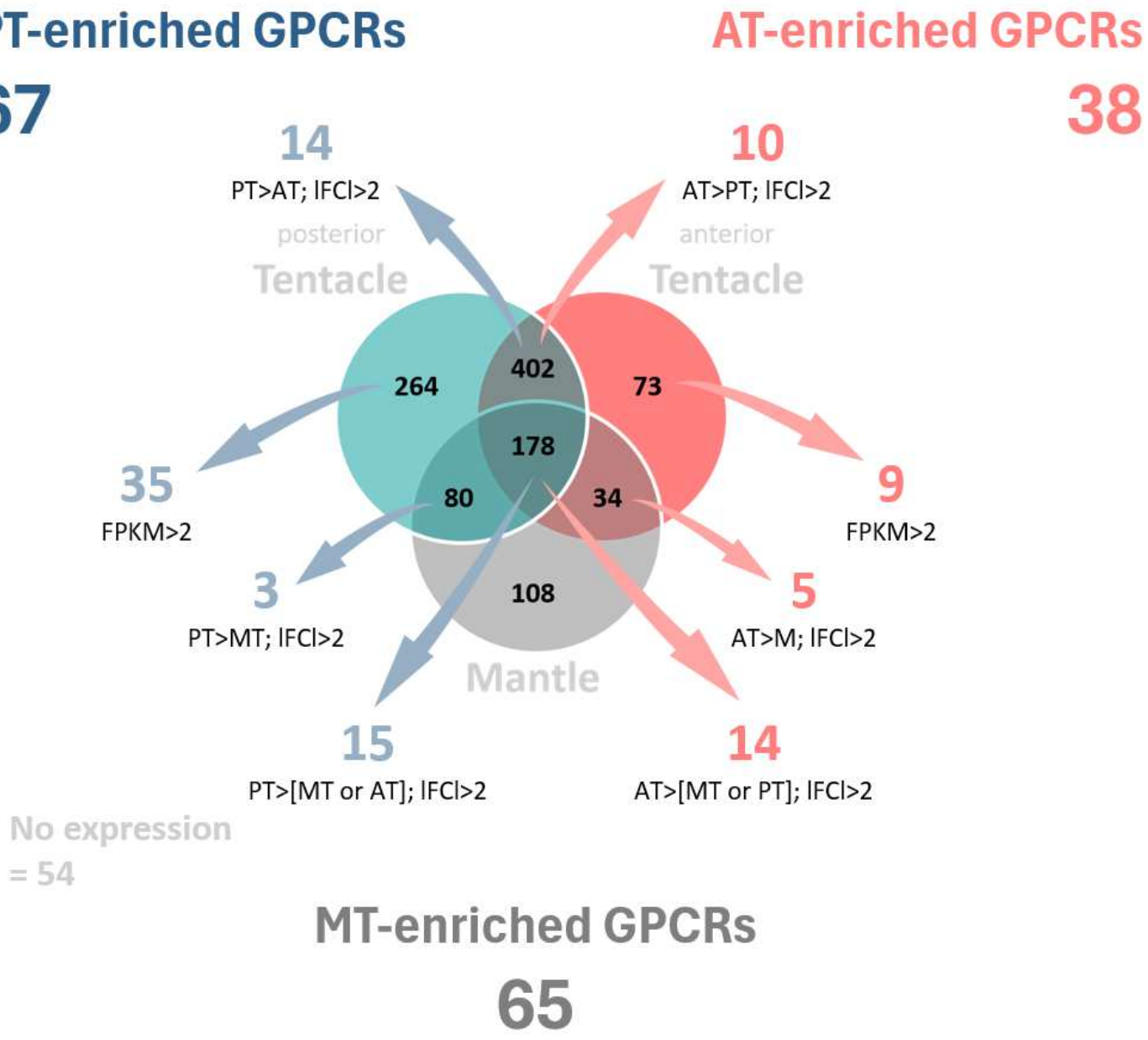


Figure 2. Filtering and identification of tentacle-enriched G protein-coupled receptors (GPCRs) from the transcriptome dataset. Candidate GPCRs were filtered through sequential analyses, including transcript annotation, transcript abundance by FPKM, and differential expression analysis by FC in the three different tissues, posterior tentacles (PT), anterior tentacles (AT), and mantle tissue (MT), resulting in the identification of putative chemosensory GPCRs enriched in tentacular tissues. Numbers within the Venn diagram indicate the number of all GPCRs expressed in the corresponding tissue categories. Numbers at the ends of the arrows outside the Venn diagram represent tissue-enriched GPCRs that met the selection criteria indicated beneath each value. The details of the MT-enriched GPCRs are not shown here. Corresponding gene lists and nucleotide sequences are provided in Supplementary Data 3.

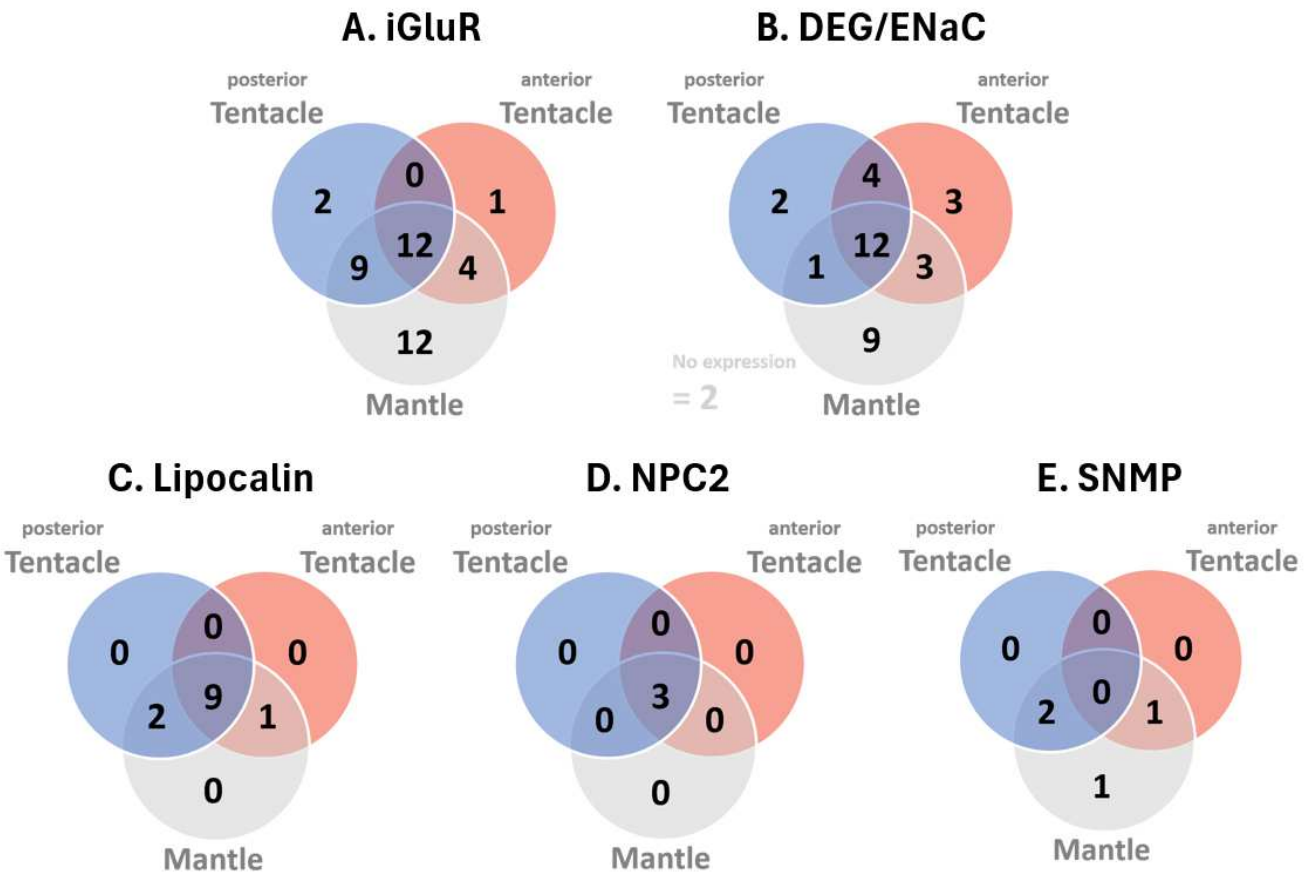


Figure 3. Tissue distribution of non-GPCR chemosensory candidate gene families in *Deroceras reticulatum*. Venn diagrams illustrate overlapping and tissue-exclusive transcripts across posterior tentacle, anterior tentacle, and mantle transcriptomes. **(A)** Ionotropic glutamate receptors (iGluRs) predominantly distributed in ubiquitous and mantle-containing profiles. **(B)** Degenerin/amiloride-sensitive sodium channels (DEG/ENaCs) distributed broadly across all domains. **(C)** Lipocalins and **(D)** Niemann-Pick type C2 proteins (NPC2) concentrated entirely within the shared universal core. **(E)** Sensory neuron membrane proteins (SNMPs) restricted to mantle-containing coordinates and absent from the shared core. Corresponding gene lists and nucleotide sequences are provided in Supplementary Data 4.

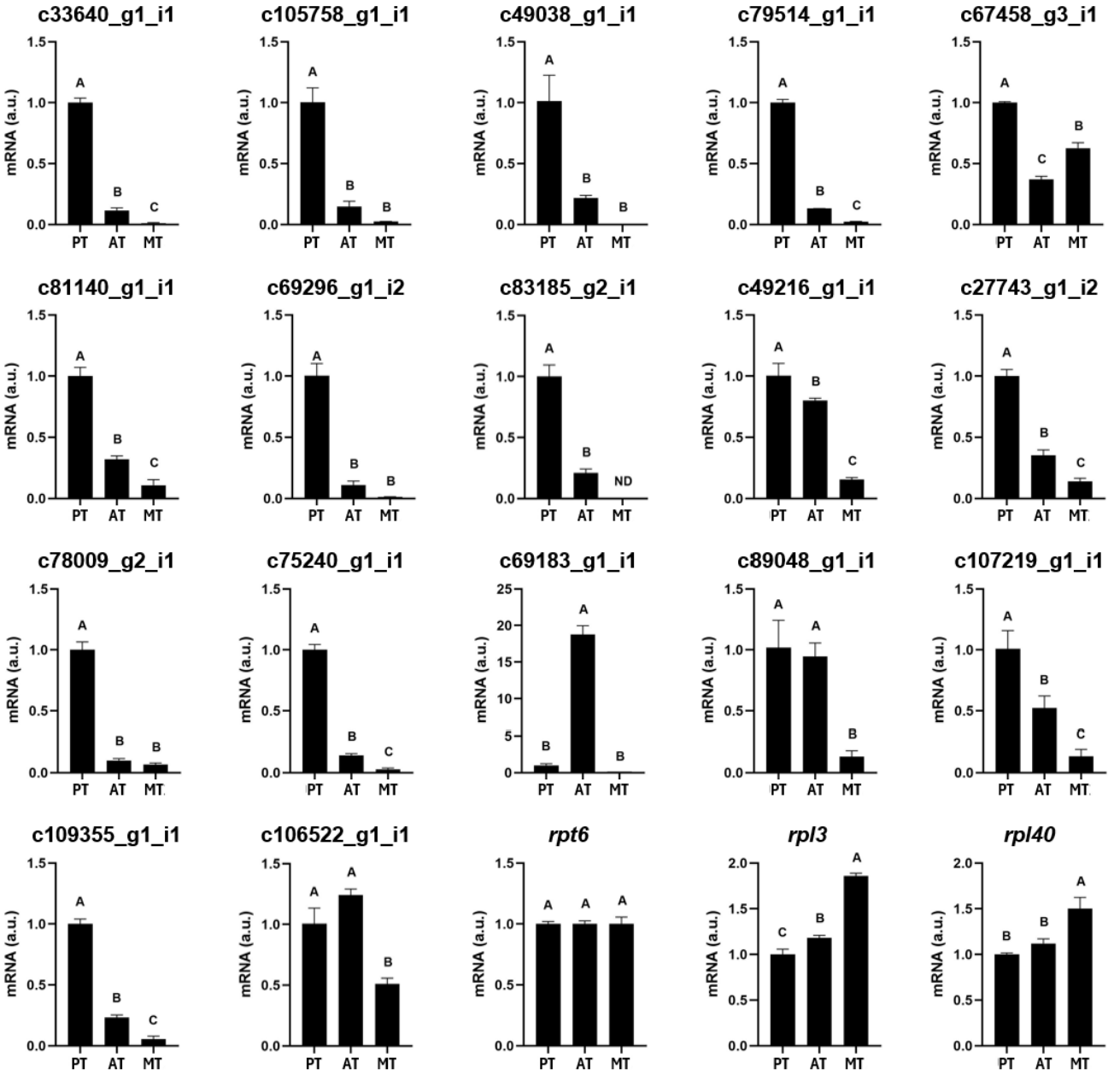


Figure 4. Relative expression levels of selected GPCR genes in the three tissues of *Deroceras reticulatum*. The relative expression levels of 17 candidate G protein-coupled receptor (GPCR) transcripts and three reference genes (*rpt6*, *rpl3*, and *rpl40*) were evaluated by qRT-PCR in posterior tentacles (PT), anterior tentacles (AT), and mantle tissue (MT). Candidate transcripts were selected based on tissue-specific expression patterns identified by RNA sequencing. Differentially expressed genes and control genes identified by RNA-seq were evaluated for relative abundance using qRT-PCR. These empirical evaluations revealed that 14 GPCR genes are highly expressed in PT, compared to AT and MT, while one GPCR (c69183_g1_i1) is exclusively highly expressed AT and two GPCRs (c89048_g1_i1 and c106522_g1_i1) are equally expressed in both PT and AT. Signal was normalized using *rpt6*. Means of three technical replicates are shown with standard-deviation error bars. Statistically significant differences are marked by different letters ($p < 0.05$), as determined by Tukey's HSD multiple comparisons test.

Supplementary Files

This is a list of supplementary files associated with this preprint. Click to download.

- Table1.docx
- Table2.docx
- SD4NonGPCRDEG.xlsx
- SD3GPCRDEG.xlsx
- SD2Top30genes.pdf
- SD1RNAseqstats.pdf
- SD5qRTPCR.pdf